

Skeletal Development in the Chinese Soft-Shelled Turtle *Pelodiscus sinensis* (Testudines: Trionychidae)

Marcelo R. Sánchez-Villagra,^{1*} Hendrik Müller,^{1,2} Christopher A. Sheil,³ Torsten M. Scheyer,¹ Hiroshi Nagashima,⁴ and Shigeru Kuratani⁴

¹Paläontologisches Institut und Museum, Universität Zürich, Karl Schmid-Strasse 4, Zürich 8006, Switzerland

²Institut für Spezielle Zoologie und Evolutionsbiologie mit Phyletischem Museum

Friedrich-Schiller-Universität Jena, Erbertstr. 1, D-07743 Jena, Germany

³Department of Biology, John Carroll University, University Heights, Ohio 44118

⁴Laboratory for Evolutionary Morphology, Center for Developmental Biology, RIKEN Kobe 650-0047, Japan

ABSTRACT We investigated the development of the whole skeleton of the soft-shelled turtle *Pelodiscus sinensis*, with particular emphasis on the pattern and sequence of ossification. Ossification starts at late Tokita-Kuratani stage (TK) 18 with the maxilla, followed by the dentary and prefrontal. The quadrate is the first endoskeletal ossification and appears at TK stage 22. All adult skull elements have started ossification by TK stage 25. Plastral bones are the first postcranial bones to ossify, whereas the nuchal is the first carapacial bone to ossify, appearing as two unstainedanlagen. Extensive examination of ossification sequences among autopodial elements reveals much intraspecific variation. Patterns of ossification of cranial dermal elements are more variable than those of endochondral elements, and dermal elements ossify before endochondral ones. Differences in ossification sequences with *Apalone spinifera* include: in *Pelodiscus sinensis* the jugal develops relatively early and before the frontal, whereas it appears later in *A. spinifera*; the frontal appears shortly before the parietal in *A. spinifera* whereas in *P. sinensis* the parietal appears several stages before the frontal. Chelydrids exhibit an early development of the postorbital bone and the palatal elements as compared to trionychids. Integration of the onset of ossification data into an analysis of the sequence of skeletal ossification in cryptodirans using the event-pairing and Parsimov methods reveals heterochronies, some of which reflect the hypothesized phylogeny considered taxa. A functional interpretation of heterochronies is speculative. In the chondrocranium there is no contact between the nasal capsules and planum suprasetale via the sphenethmoid commissurae. The pattern of chondrification of forelimb and hind limb elements is consistent with a primary axis and digital arch. There is no evidence of anterior condensations distal to the radius and tibia. A pattern of quasi-simultaneity is seen in the chondrogenesis of the forelimb and the hind limb. *J. Morphol.* 270:1381–1399, 2009. © 2009 Wiley-Liss, Inc.

KEY WORDS: ossification sequence; heterochrony; skeleton; growth; Parsimov; Cryptodira

INTRODUCTION

Turtles are unique among living tetrapods in that they possess a box-like shell that is formed by dorsal and ventral parts (the carapace and

plastron), which together cover most of the body in the majority of taxa. The turtle shell has been considered a textbook example of a morphological novelty (Gilbert et al., 2001). However, is not just the shell of turtles that is remarkable in its morphology, most other elements are also highly modified.

Among recent turtles, soft-shelled turtles (Trionychidae) are arguably the most distinctive and morphologically derived group, characterized by a greatly reduced shell covered by a thick, leathery epidermis. Scheyer et al. (2007) reported a laminated structure of bone histology within Trionychidae, and demonstrated that this is unique among turtles. The postcranial skeleton also shows peculiarities, such as an increased phalangeal formula (Richardson and Chipman, 2003). The living diversity of trionychids includes about 14 genera and 30 species (Meylan, 1987; Engstrom et al., 2004; Bickham et al., 2007; Fritz and Havaš, 2007). Among them, the Chinese soft-shell turtle *Pelodiscus sinensis* is one of the best known forms, and it is commercially exploited (Ginsberg, 2002; Ministry of Agriculture, Forestry and Fisheries of Japan, 2007). Additionally, this species has become a major subject of study in developmental and

Additional Supporting Information may be found in the online version of this article.

Contract grant sponsor: Swiss National Fund; Contract grant number: 3100A0-116013; Contract grant sponsors: Fonds zur Förderung des akademischen Nachwuchses (FAN), des Zürcher Universitätsvereins (ZUNIV).

*Correspondence to: Marcelo R. Sánchez-Villagra, Paläontologisches Institut und Museum, Universität Zürich, Karl Schmid-Strasse 4, Zürich 8006, Switzerland. E-mail: msanchez@pim.uzh.ch

Received 21 December 2008; Revised 1 May 2009; Accepted 1 May 2009

Published online 15 June 2009 in Wiley InterScience (www.interscience.wiley.com)
DOI: 10.1002/jmor.10766

molecular investigations of the origin of the turtle shell (Kuraku et al., 2005; Nagashima et al., 2005; Ohya et al., 2005). In spite of this and the early description of the adult anatomy of *Pelodiscus* by Ogushi (1911) and of several aspects of shell development by Cherepanov (1995), there are no data on skeletal formation in this species. Sheil (2003) described skeletal development in the trionychid *Apalone spinifera*, and there are similar works on other cryptodires (*Chelydra serpentina*: Rieppel, 1993a; Sheil and Greenbaum, 2005; *Macrochelys temminckii*: Sheil, 2005; *Trachemys scripta*: Sheil and Portik, 2008), and the pleurodire *Phrynops hilarii* (Bona and Alcalde, 2009). Here, we provide a summary of developmental events with focus on those stages that are most informative for the onset and early ossification of skeletal elements. We also provide the first quantitative examination of skeletal heterochrony in cryptodiran turtles, which future studies can expand and compare using similar analyses of other amniote clades (Maxwell and Harrison, 2008; Sánchez-Villagra et al., 2008a; Weisbecker et al., 2008). Considering the importance of developmental data in the interpretation of new fossils documenting early turtle evolution (Li et al., 2008; Reisz and Head, 2008), our study also delivers relevant data for future comparative analyses.

MATERIALS AND METHODS

Collection of Embryos and Descriptive Morphology

Eggs of *Pelodiscus sinensis* were obtained from a commercial turtle farm and incubated in the laboratory, as described by Tokita and Kuratani (2001). Embryos were removed from their eggs at regular intervals to sample as much of the ontogenetic sequence as possible, and each specimen was fixed in Bouin's fixative and 20% formalin, and developmental stages were determined by reference to the staging criteria of Tokita and Kuratani (2001). Embryos were cleared and double-stained for bone and cartilage following standard procedures (Taylor and Van Dyke, 1985). Retention of stain in bone and cartilage generally was excellent; however, in some cases early bone formation was not indicated by Alizarin Red stain, but rather by appearance as a faint structure with a distinct surface texture (Rieppel, 1993a; Sheil, 2003). The latter scenario was not considered evidence of first ossification, but rather, earliest ossification was determined to be the earliest stage at which Alizarin Red was retained for that element. There is a possibility of de-calcification due to the acetic acid contained in the Alcian blue solution. To study ossification only, ideally one should prepare the specimens stained only by Alizarin, with no exposure to acid for cartilage staining or hydrogen peroxide for de-pigmentation. Histological sections also show ossification at earlier stages and in a more reliable way (Vogel, 1972). But as all the specimens were treated with the same method and we are primarily interested in recording sequences of ossification, we can define the start of ossification with appearance of red staining and compare stages with no bias introduced in the analysis of heterochrony (Sánchez-Villagra, 2002). For the comparison of ossification across species presented here, only the relative timing or sequences are important, and for that reasons the differences in technical approaches across studies do not affect our study.

Fifty-one specimens ranging from stages 15–27 (hatchling), as well as two large juveniles were examined (Supporting Information). These specimens formed the basis of comparison for the descriptive morphology, as well as documentation of ossification sequences. We describe the chondrocranium based primarily on specimens from stages 19–21 (specimens 015, 019, 020, and 021) and base the illustrations on a stage-20 specimen (019). This description is part of ongoing studies by one of us (C.A.S.) and future comparisons and phylogenetic analyses will be based on comparisons with other turtle taxa (Tulenko and Sheil, 2006).

Comparisons of Ossification Sequence Through Ontogeny

Specimens were examined and scored for the presence or absence of individual cranial and postcranial skeletal elements to elucidate the ontogenetic sequence of ossification events for the entire skeleton. In total, 76 individual ossification events were identified and summarized for *P. sinensis*; however, to enable a broader comparison with data from the literature for other taxa (see below), we reduced these ossification events to a total of 66 cranial and postcranial events that were common to all taxa. The reduction in event numbers involved postcranial ossification events in which we grouped single ossifications into larger categories. For example, all metatarsals were grouped together and onset of ossification for this group was considered to occur at the first ossification of any metatarsal within this group. Similar procedures were followed for: the neural arches and centra of the cervical, thoracic, sacral, and caudal regions; ribs of the trunk and sacral region; serial elements of the manus and pes (e.g., metacarpals/tarsals, phalanges, and proximal and distal autopodial elements); and costals. We compared our data for *P. sinensis* with those of six additional taxa obtained from the literature: Spiny soft-shell turtle (*Apalone spinifera* [Sheil, 2003]); common and alligator snapping turtles (*Chelydra serpentina* [Sheil and Greenbaum, 2005] and *Macrochelys temminckii* [Sheil, 2005]); American alligator (*Alligator mississippiensis* [Rieppel, 1993b]); Japanese quail (*Coturnix japonica* [Nakane and Tsudzuki, 1999]); and common wall lizard (*Lacerta vivipara* [Rieppel, 1992]).

A data matrix was constructed in which the relative timing of each ossification event was compared individually to all other ossification events. The relative timing of all nonredundant event pairs were scored according to whether a given ossification event occurred before (score 0), simultaneously (score 1), or after (score 2) the ossification event to which it was compared. This resulted in a final matrix with 2145 event pairs (i.e., characters) with character states 0, 1 or 2. Several elements are considered unique to turtles (e.g., hyo-, hypo-, xiphi-, epi-, and entoplastron, nuchal, acromion, neurals, and costals) and were coded as unknown in the other taxa (i.e., score "?"). The postorbitofrontal of *Lacerta vivipara* was coded in place of the postorbital of turtles, assuming homology of the ossification center initiating in both elements. Because of the highly derived limb skeleton in birds, several events were coded as unknown in *Coturnix japonica* (e.g., proximal and distal carpals, centrals of the manus, and pisiform); similarly, in the skull the postorbital and epipterygoid were scored as "?" because these elements are known to be absent in birds (Zusi, 1993). Elements that are present in the nonturtle taxa but absent in turtles were not considered here; this was done to guarantee the most inclusive dataset from which comparisons of ossification events could be inferred. The evolutionary relationship of turtles to other amniotes remains controversial (e.g., Rieppel, 1995, 2004; Rieppel and de Braga, 1996; Hedges and Poling, 1999; Meyer and Zardoya, 2003; Müller, 2003; Hill, 2005; Werneburg and Sánchez-Villagra, 2009). Several recent studies (e.g., Zardoya and Meyer, 2001; Jiang et al., 2007) have supported the hypothesis that turtles are the sistergroup of Archosauromorpha (crocodilians and birds, here represented by *Alligator mississippiensis* and *Coturnix japonica*). The phylogenetic hypothesis on which subsequent analyses of evolutionary changes in ossification sequences (heterochrony) were based is shown in Figure 1.

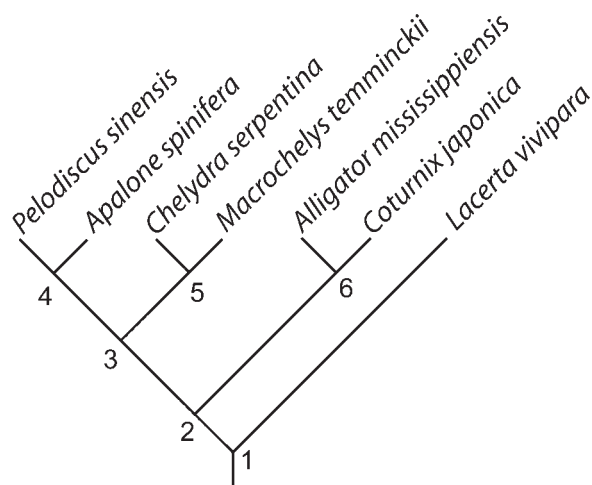


Fig. 1. Phylogenetic hypothesis upon which the Parsimov analyses were performed.

Parsimov Analysis

Parsimov (Jeffery et al., 2005) is a parsimony-based method of analyzing ontogenetic data. The program identifies the sequence of events that requires the fewest number of ad hoc hypotheses for timing changes for individual elements within a sequence and across a cladogram. We used Parsimov to identify character changes on all branches of the reference cladogram (see Fig. 1) and generate apomorphy lists for internal and terminal branches (Maddison and Maddison, 2006). The methods of optimizing these data are tied to the model of evolution assumed (ACCTRAN, accelerated or DELTRAN, delayed evolution of characters) and can impact the results of the analyses. We applied a conservative approach to our analyses, by examining a strict consensus of results of ACCTRAN and DELTRAN optimizations (Sánchez-Villagra et al., 2008a; Weisbecker et al., 2008). The heterochronic changes in ossification sequences are listed in the Supporting Information to this article.

Most event-pair ties are probably an artifact of sampling error in cases where the rate of ossification or appearance of bones exceeds the rate of progress through defined developmental stages, thereby leading one to identify multiple events that occur at a single developmental stage (Velhagen, 1997). To briefly consider the effect of event-pair ties on this analysis, a second analysis of the dataset was performed in which event-pair ties were converted from "1" to "?" (scored as unknown timing).

Limb Chondrogenesis

We examined early limb chondrogenesis in *Pelodiscus sinensis* based on three stages (16, 17, 18) that document the general outline in the development of the primary axis and the digital arch (Shubin and Alberch, 1986; Richardson et al., 2009). Terminology follows Burke and Alberch (1985); numbering of centralia is avoided given the uncertain homologies of specific elements in that area of the autopodials (Gaffney, 1990).

RESULTS

Ossification Patterns of the Skull and Jaw (see Fig. 2)

Maxilla. The maxilla is one of the first elements to ossify and is first visible in a late stage-18 embryo as a small, elongated, unstained plate-like structure anterior and ventral to the eye. By stage

19 the maxilla retains considerable Alizarin red stain, and at stage 21 it is triangular in shape and forms the anteroventral quarter of the orbit, whereas the ventral margin contacts most of the upper margin of the mouth. A prefrontal process extends dorsally nearly to the level of the dorsal margin of the nasal capsule; however, the maxilla and prefrontal do not articulate. A shallow but prominent labial ridge extends along the length of this bone, and a shelf-like pars palatina of the maxilla extends medially along the palatal region. By stage 23 the dorsal process of the maxilla laterally invests the ventral process of the prefrontal. The palatal shelf has expanded slightly, especially at the posterior end of the maxilla.

Prefrontal bone. The prefrontal bone is first visible as a relatively robust but unstained triangular element immediately anterior to the eye, just above the antorbital plane of cartilaginous nasal capsule. This element is stained from stage 20 on, and by stage 21 it has developed a slender dorsal process that extends posterodorsally almost to the level of the planum supraseptale, and forms part of the orbit. Ventrally, two relatively weakly developed processes extend medially and laterally along the posterior border of the nasal capsule. By stage 23 the medial and lateral ventral processes have fused into a single shelf that forms the anteroventral border of the orbit, separating the orbit and the nasal capsule. The dorsal process of the prefrontal widely overlaps the anterior part of the frontal.

Parietal bone. The parietal bone is first apparent as an unstained triangular plate lateral to the brain and posterior to the eye in a stage-20 embryo, and very weakly stained in a late stage-20 embryo. At stage 21 the parietal is well stained, apart from a weakly stained descending process. By stage 23 the parietal is only slightly expanded and overlaps with the posterior end of the frontal, while extending posteriorly to above the anterior surface of the otic capsule.

Squamosal bone. The squamosal bone is first apparent at stage 20, and forms an unstained, anteriorly-directed triangular element that covers the dorsal aspect of the otic capsule and extends slightly beyond the otic capsule in a short, posteriorly-directed process. It is weakly stained in a late stage-20 embryo. Otherwise, this is a well-stained element from stage 21 on.

Jugal bone. The jugal bone is first present but unstained in stage 20 embryos, and forms a thin, slender bar at the ventroposterior border of the orbit. By stage 21 it is triangular in shape, with a concave dorsal edge that forms the posteroventral margin of the orbit. It is positioned ventrolateral to the parietal.

Palatine bone. The palatine bone is first present by stage 21 and forms a small plate-like element that is subtriangular to semilunar in

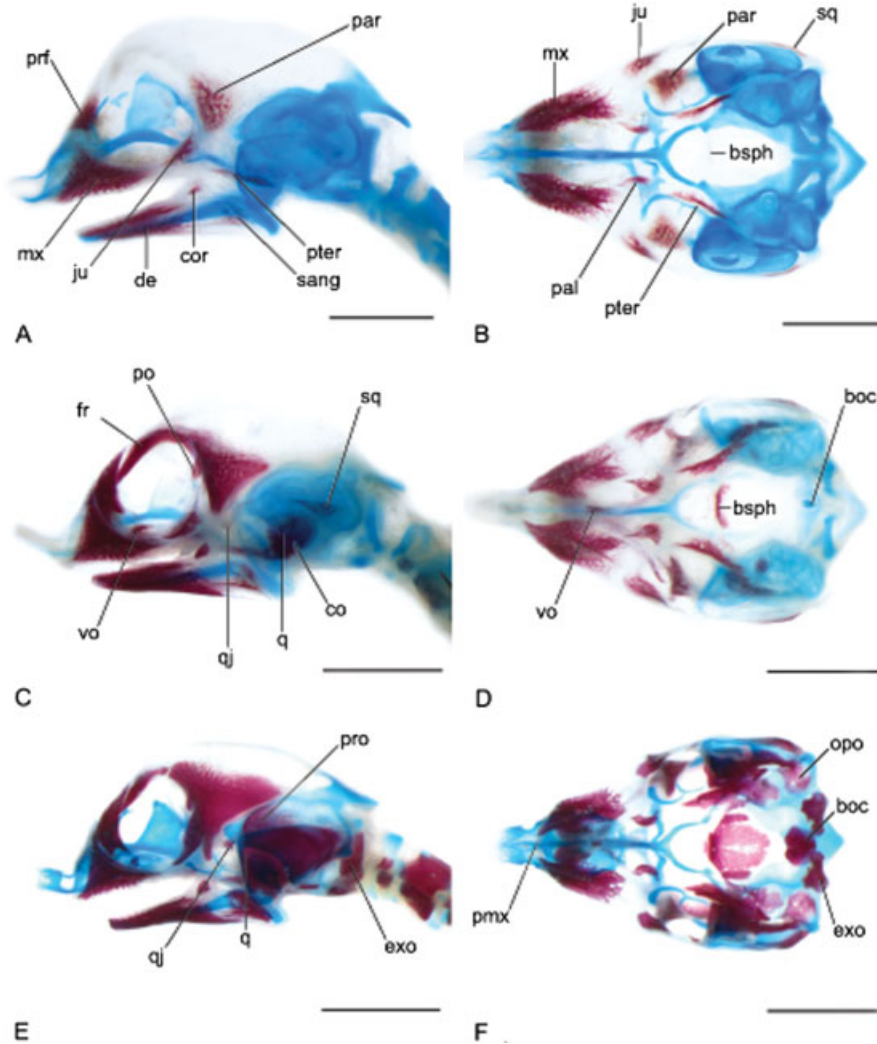


Fig. 2. Lateral (A, C, E) and ventral (B, D, F) views of the developing skull of *Pelodiscus sinensis*, as shown by three cleared and double-stained embryonic specimens. Specimens depicted are at stages TK 21 (A, B, specimen 019), TK 23+ (C, D, 027) and TK 25 (E, F, 112). Abbreviations: boc, basioccipital; bsp, basiphosph; cor, coronoid; exo, exoccipital; fr, frontal; ju, jugal; mx, maxilla; opo, opisthotic; pal, palatine; par, parietal; pmx, premaxilla; po, postorbital; prf, prefrontal; pter, pterygoid; q, quadrate; qj, quadratojugal; sang, surangular; sq, squamosal; vo, vomer. Scale 2 mm.

shape, with the concave side facing laterally. At stage 23 shape and position of the palatine are essentially similar, although the element is slightly larger.

Pterygoid. The pterygoid is present as a slender, elongated plate-like element in a stage-21 embryo, and extends along the ventrolateral margin of the trabecula from slightly behind the level of the pterygoid process of the palatoquadrate to just posterior the level of the lower jaw articulation. This element expands anteriorly by stage 23.

Frontal bone. The paired frontal bones are present in stage-20 and -21 embryos as slender, bar-like elements that form the anterodorsal margin of the orbit. In each the anterior terminus is positioned medial to the dorsal process of the prefrontal. By stage 23 each frontal is stained and

invested dorsally by the posterior terminus of the prefrontal, whereas the posterior terminus of each invests the anterior terminus of the parietals.

Premaxilla. The premaxillae fuse early, and are first apparent by stage 21 as a very small, unstained plate that is oriented transversely between the anterior termini of the maxillae, below the nasal septum. This element is stained from late stage 23 onwards.

Postorbital bone. The postorbital bone is first present at stage 23 as a small, oval plate at the posterior margin of the orbit, lateral to the parietal. Bilateral asymmetry is apparent in two stage-23 specimens, but otherwise these elements are well stained in all specimens older than this stage.

Vomer. The vomer first appears as an unpaired, unstained element that is small, triradiate, and

positioned ventral to the medial interorbital septum, at the level of the prefrontal. This element may be absent in a stage-22 embryo, but otherwise is well stained from stage 23 onwards.

Quadratojugal bone. The quadratojugal bone is first apparent as a small, unstained triradiate structure in a stage-21 embryo, and is positioned posterior to the jugal and lateral to the anterodorsolateral margin of the palatoquadrate. At stage 23 the quadratojugal is stained on one side only in a single embryo and stained on both sides in another embryo of the same stage; otherwise this element is stained in all specimens older than stage 23.

Quadrate. The quadrate ossification is first apparent as a thin, unstained perichondral layer of bone around the incisura columella auris. It is ossified from stage 22 onwards and has replaced most of the medial wall of the palatoquadrate by stage 23.

Basisphenoid. The basisphenoid is first seen in a stage-21 embryo as an unstained, thin, vertically positioned plate in the pituitary-basiscranial fenestra, at the level of the area articularis of the quadrate cartilage. It seems to have a paired anlage; however, in a stage-22 embryo, an unpaired element is ossified. By late stage 24, the basisphenoid covers the posterior part of the pituitary-basiscranial fenestra; nearly the entire opening of this fenestra is covered by late stage 25.

Columella. The columella first appears as a thin, unstained layer of perichondral bone around its shaft. It is well stained in all embryos by stage 22.

Basioccipital bone. The basioccipital bone is present as a small, medial ossification of the basal plate in stage-23 embryos. It is apparently absent in a single early stage-24 embryo but otherwise is present in all embryos by stage 24.

Exoccipital bone. The Exoccipital bone is First Present at Stage 24

Prootic and opisthotic bones. The prootic bone is also first present in most stage-24 embryos as a perichondral ossification of the anterior part of the otic capsule, medial to the palatoquadrate-quadrate. The opisthotic bone is first present by stage 24, and is present in all but one of the examined embryos. It forms in part as a small, perichondral ossification of a small cartilaginous process (*processus paraoccipitalis*, Sheil, 2003) at the posteroventral margin of the palatoquadrate cartilage.

Supraoccipital bone. The supraoccipital bone is first present in late stage-24 embryos and nearly all stage-25 specimens. It forms as a thin perichondral ossification of the posterolateral edge of the tectum synoticum medial to the otic capsules. In all specimens, it develops from a pair of ossification centers that fuse along the midline by late stage 25.

Epipterygoid. The epipterygoid is present in some stage-25 embryos, although most embryos of this stage lack any ossification of the ascending process of the palatoquadrate cartilage. It also is absent or unstained in three stage-26 embryos, but otherwise is stained in all specimens by stage 26.

Dentary. The dentary is one of the earliest elements to ossify and is first weakly indicated as an unstained, rod-like structure in a late stage-18 embryo, where it spans along the ventrolateral margin of the anterior half of Meckel's cartilage. It is stained in embryos of stage 19 and older. At stage 21 the dentary covers the entire anterior lateral half of Meckel's cartilage and extends posteriorly along the ventral edge of this cartilage to a level just anterior of the area articularis. The dentary has developed a distinct labial ridge by stage 21.

Surangular bone. The surangular bone is first present in a stage-19 embryo, and is very weakly indicated as an unstained, short and slender bar on the ventrolateral margin of the posterior part of Meckel's cartilage just anterior to the area articularis. It is weakly stained in a late stage-20 embryo and has formed a triangular plate that covers the lateral aspect of the posterior part of Meckel's cartilage, lateral to the area articularis. It articulates broadly with the dentary by stage 24.

Coronoid. The coronoid is first present in a late stage-20 embryo as a tiny plate posterior to the dentary, nearly at the level of the parietal. It is well stained in a stage-21 embryo, where it forms a small, subtriangular plate posterior to the dorsal margin of the dentary.

Angular bone. The angular bone is first present in a stage-21 embryo, where it forms a weakly-stained, narrow rod that lies at the ventromedial margin of the posterior half of Meckel's cartilage, just anterior to the lower jaw articulation.

Prearticular and articular bone. First indication of the prearticular bone is apparent in a stage-21 embryo, where it forms a small, unstained triangular plate at the medial surface of Meckel's cartilage, just anterior to the area articularis. It is absent in a stage-22 embryo, but otherwise is stained from stage 23 on. The endochondral articular bone is present in most stage-25 embryos, and all but one specimen by stage-26.

Ossification Patterns of the Postcranial Axial Skeleton

Cervical vertebrae (see Fig. 3). The cervical region is composed of eight highly mobile vertebrae, with those of the posterior region being slightly broader than those positioned more anteriorly. The axis is similar in shape to cervical vertebrae III-VIII, whereas the atlas diverges strongly in morphology, with a short centrum and bipartite,

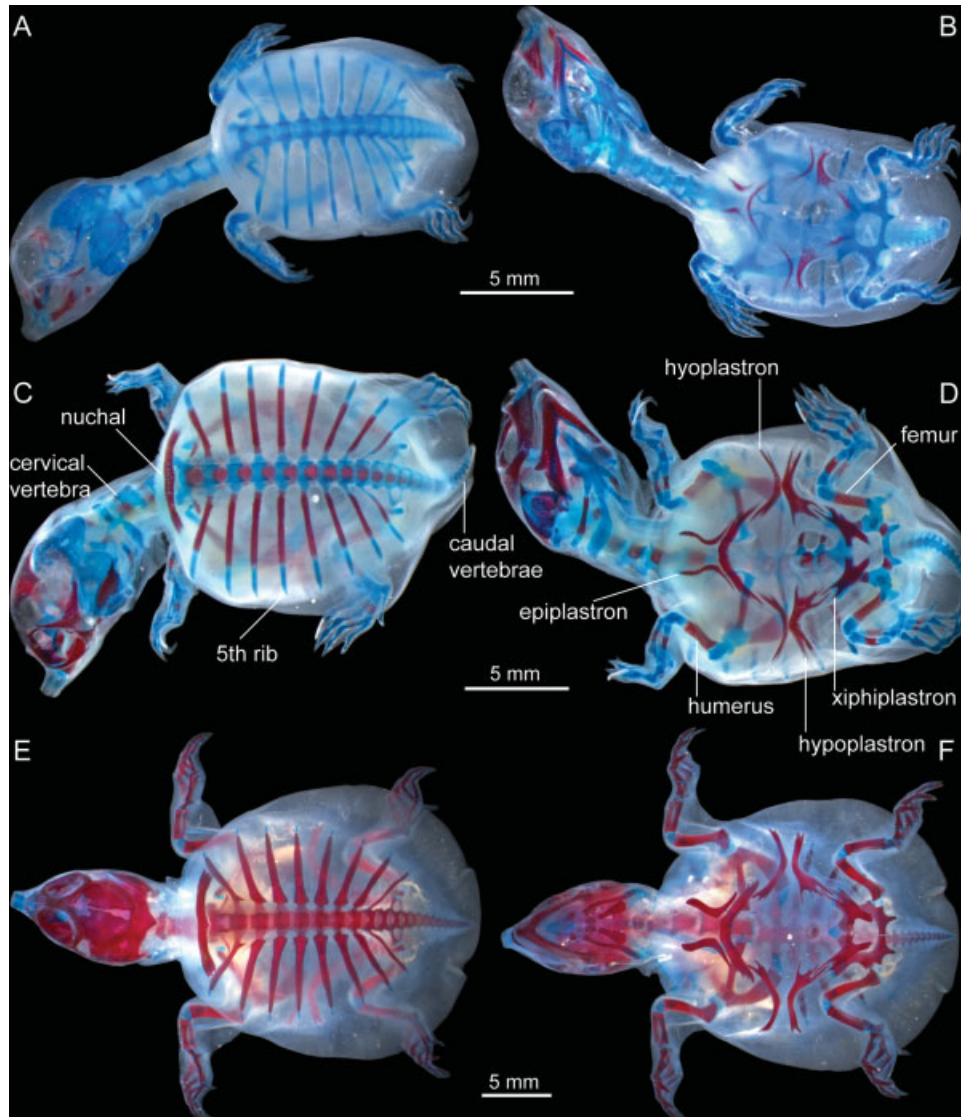


Fig. 3. Skeletal sequential development in three cleared and double-stained embryonic specimens of *Pelodiscus sinensis*. The specimens are shown in dorsal (A, C, E) and ventral view (B, D, F). (A, B) Specimen (019) at stage 21. The retention of Alizarin Red is strongest in the anterior part of the head and the plastron. In the carapace, the ossification of the nuchal is initiated. (C, D) Specimen (101) at stage 24-. Ossifications are now also found in the posterior part of the head, as well as in all postcranial regions. (E, F) Specimen (132) at stage 27. The specimen, which was near hatching, shows the highest degree of ossification of all specimens under study. The cranial and postcranial elements are well ossified, although the characteristic shell is virtually nonexistent yet at this stage.

bow-shaped neural arch. A posterior–anterior gradient in ossification of the cervical vertebrae is apparent in the centra and neural arches. The trend to direction of ossification was inferred by relative degrees of ossification in the cervical vertebrae. Retention of Alizarin red was recorded in the cervical centra at stage 19, whereas ossification of the cervical arches was first observed by early stage 24.

Dorsal vertebrae (Figs. 3 and 4). Ten presacral dorsal vertebrae are present in the carapacial disc of *P. sinensis*. All dorsal vertebrae are akinetic and become part of the neural series, which in

later stages of development form the seven neurals discussed by Ogushi (1911:fig. 8). The first dorsal vertebra diverges in morphology from the more posterior dorsals in having two prominent prezygapophyses that curve anterior and ventrally to articulate with the postzygapophyses of cervical vertebra VIII, to enable the typical S-shaped flexing of the cryptodiran neck, that is highly developed in the Trionychidae (Dalrymple, 1979). The length of the dorsal centra decreases in an anterior–posterior trend, and an anterior–posterior trend of ossification is recognized in the dorsal centra and neural arches. Similar to the cervical

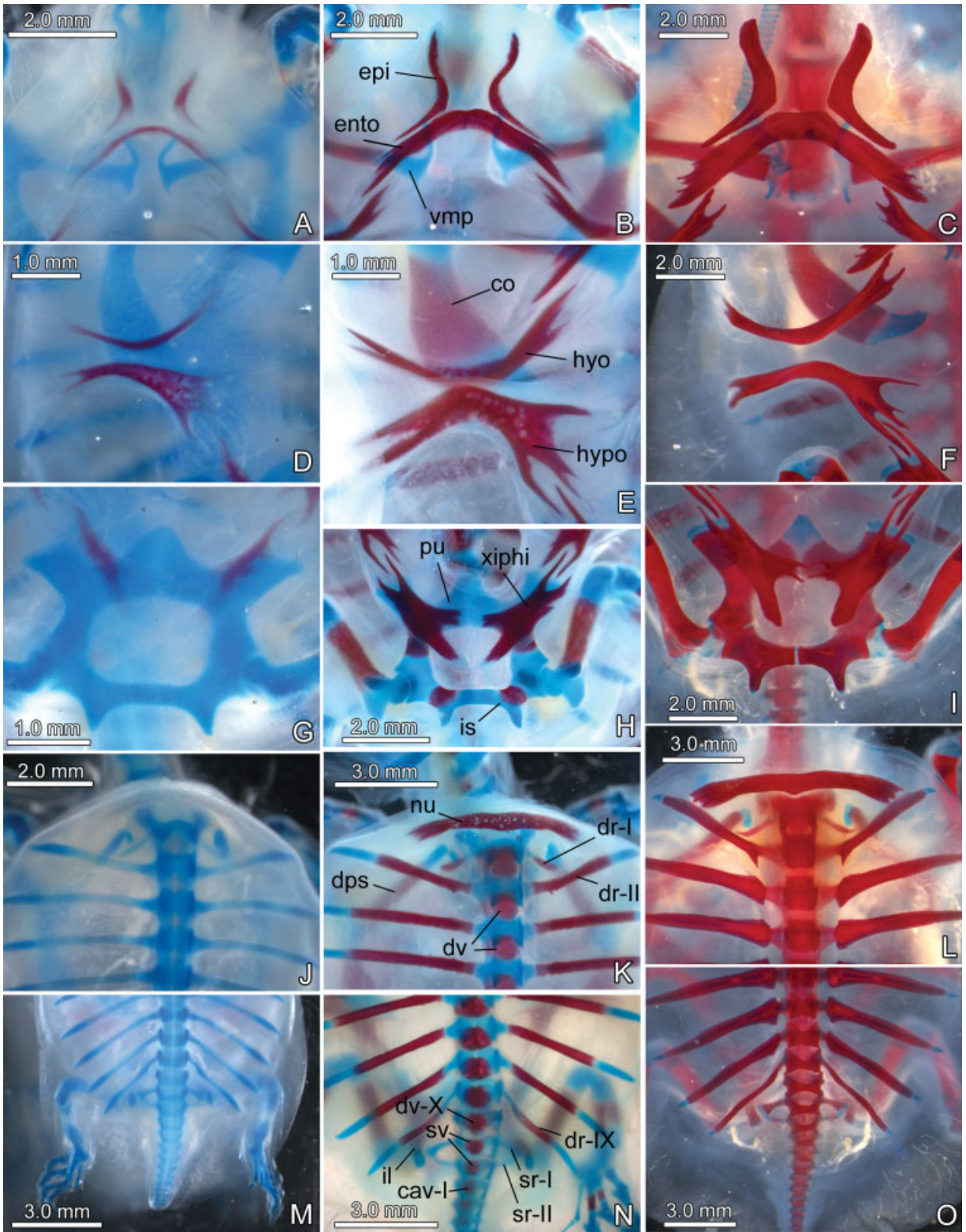


Fig. 4. Representative close-ups of the sequential development and ossification of selected postcranial elements of *Pelodiscus sinensis*. All shell elements and endoskeletal bones are shown in an early (stage 19), an intermediate (stage 21) and a late embryonic stage (stage 27) of development. (A–C) Epiplastra, entoplastron and ventromedial process of the scapula in ventral view. (D–F) Right hyoplastron, hypoplastron and posterior part of the coracoid in ventral view. (G–I) Xiphiplastra and the ischia and pubes of the pelvic girdle in ventral view. (J–L) Anterior part of the carapace (i.e., nuchal bone, anterior dorsal vertebrae; first four pairs of dorsal ribs) in dorsal view. Ventral to dorsal rib I and II the dorsal process of the scapula is visible. (M–O) Posterior part of the carapace and the proximal part of the tail in dorsal view. Abbreviations: cav, caudal vertebra; co, coracoid; dps, dorsal process of scapula; dr, dorsal rib; dv, dorsal vertebra; ento, entoplastron; epi, epiplastron; hyo, hyoplastron; hypo, hypoplastron; il, ilium; is, ischium; nu, nuchal; pu, pubis; sv, sacral vertebra; sr, sacral rib; vmp, ventromedial process of scapula; xiphi, xiphiplastron.

vertebrae, the centra of all dorsal vertebrae begin ossification much earlier (by stage 19) than the dorsal neural arches (by early stage 24).

Sacral vertebrae and ribs (Figs. 3 and 4). There are two sacral vertebrae, each articulating with a corresponding sacral rib. The sacral centra and neural arches generally resemble those of the dorsal region. The lateral terminus of the first sacral rib expands anteroposteriorly, whereas that of the second sacral rib is relatively straight and rod-like. In well-ossified specimens (e.g., hatchlings), rib morphology does not change markedly from earlier developmental stages; the first sacral rib develops a broad lateral cartilaginous articular facet, and the second sacral rib only a marginal one. All specimens studied still lacked articulation of the sacral ribs and the ilium. Ossification of the sacral centra was inferred on the basis of surface texture by stage 22, and by stage 24– ossification was well under way. Alizarin red was found in the sacral arches at stage 24+. Sacral ribs demonstrated a strong divergence in the onset of ossification. First retention of Alizarin red was noted by stage 25– in sacral rib I, whereas similar retention was found only at stage 27– in sacral rib II. No such indication was found in the onset of ossification in the sacral centra and arches, which appear to ossify simultaneously.

Caudal vertebrae (Figs. 3 and 4). Generally, 13 caudal vertebrae are recognized, however, several individuals were found to have 14 caudal anlagen. In shape, the caudal centra and neural arches are indistinguishable from those of the sacral and dorsal vertebrae. The centra carry small short transverse processes, but none of the specimens studied possessed ossified transverse processes. Caudal centra and vertebral arches show an anterior–posterior gradient in ossification, but prominent individual variation was recorded among the elements of these regions. The anterior caudal centra start ossifying by stage 24–. Complete ossification of all caudal centra was found only in a single stage-27 specimen (129). The anterior caudal arches were ossified at stage 24+.

Dorsal ribs and carapace (Figs. 3 and 4). The nuchal bone is the first bone to ossify in the carapace, and it appears as two unstained anlagen by stage 19; ossification is present in the paired ossification centers by stage 21 (specimen 19). Although difficult to assess in the specimens due of the underlying developing vertebral arches of the posterior-most cervical and the first dorsal, there seems to be no apparent connection between the two unstained anlagen of the nuchal. Whereas a medial connection cannot be completely ruled out, we detect only two separate lateral ossification centers, instead of a single medial one (see electronic Supporting Information). With the medial connection of the two ossification centers, the nuchal develops as a boomerang-shaped element

with lateral termini that extend posterolaterally. At later developmental stages, the medial portion of the element bears a straight to slightly concave anterior margin, and a distinctly convex posterior margin. The lateral processes of the nuchal are recurved posteriorly and terminate in a thin, frayed, and irregular margin. The medial portion of the element lacks compact bone, and the spongy interior is visible. Compact cortical bone of the nuchal is well developed by stage 27, and from stage 27– onward, ossification has extended overlapping the anterior-most vertebral arches.

The dorsal ribs start as rather straight cartilaginous rods that are arranged in a fan-shaped pattern in the turtle carapace. Dorsal rib I differs from the other dorsal ribs in that it is small, thin bone that grows posteriorly from dorsal vertebra I and articulates in posthatchling specimens with the anterior margin of the dorsal rib II, thus having a curved (anteriorly concave) shape. Medially, the dorsal ribs bend ventrally to form continuous anlagen (the rib heads of later ontogenetic stages) with the centra of the dorsal vertebrae. Ossification of the dorsal ribs I–IV starts at stage 21, however, retention of Alizarin red commences at stage 22. At this stage, the dorsal rib V starts ossifying, though Alizarin red is not yet retained. By stage 24–, all dorsal ribs (I–IX) have started ossification as indicated by retention of Alizarin red. In all dorsal ribs, the ossification starts at the middle portion of the rib shafts and progresses medially and laterally. In specimen 132 (stage 27), the medial parts of the dorsal ribs II and III (articulating with the dorsal centra) appear well ossified, whereas the more posterior dorsal ribs retain some cartilage in these areas. All studied specimens retain cartilage tips at the lateral margins of the dorsal ribs II–IX, whereas the tip of dorsal rib I is already ossified at stage 24–.

There are eight pairs of costal bones forming the bony carapacial disc in *P. sinensis*. Costal I is strongly associated with dorsal rib II, but also covers the diminutive dorsal rib I, which contacts dorsal vertebra I. The more posterior costals (II–VII) are each associated with only one dorsal rib, thus the eighth costal is associated with dorsal rib IX. Costal VIII also covers the short transverse process of the tenth dorsal vertebra. This transverse process first ossified by stage 27. Initial indication of costal outgrowths from the periosteal collars of the dorsal ribs was texturally observable at stage 23 for costals I–IV. At stage 24–, all but costal VIII were ossified based on Alizarin red staining. Ossification was indicated by weak staining only from stage 26– onward in costal VIII. Similar to the associated ribs, the costal plates start to develop at intermediate positions on the ribs and continue to develop medially and laterally. Even in hatchlings, the costals remain thin laminar bony structures that have not grown far between the dorsal ribs;

therefore none of the examined specimens exhibits articulations between adjacent costal plates. There is no sign of any anlage for peripheral bones, which, as in all trionychids except *Lissemys* spp., are fully reduced in adult *P. sinensis*.

Plastron (Figs. 3 and 4). The plastral bones, none of which develops from a cartilaginous precursor, are the first to ossify in the postcranium of *P. sinensis*. At stage 18+, the paired posterior hyo-, hypo- and xiphiplastra are recognizable on the basis of textural differentiation. Alizarin red is retained in these elements at stage 19. At this stage, the anterior anlagen of the epiplastra and the median entoplastron can be seen based on textural differences and a clear retention of Alizarin red is recorded at stage 20+. Ossification generally starts at the central portions (i.e., crest-regions) of the elements and spreads into the tapering processes, respectively.

The epiplastra are crescent-shaped, concave laterally, with a broader anterior process and a sharply pointed posterolateral process. The posterior margins of the epiplastra extend parallel to, but do not articulate with, the anterolateral margins of the unpaired entoplastron. At early stages of ossification, the entoplastron is crescent-shaped, with a posterior concavity and two sharply pointed posterolateral processes. It later develops a flat anterior crest while retaining the posterior concavity and two broad posterolateral flanks. Laterally, each of the flanks shows several thin bony protrusions. The hyoplastra start ossifying as thin crescent-shaped, sharply pointed rods with anterior concavities. In later stages, the hyoplastra develop a more straight lateral portion and a plate-like medial portion. Both portions carry thin finger-like processes that extend beyond the actual bone margins. At stage 27, there are two blunt lateral protrusions and three pointed medial protrusions, with the anterior medial parts of the hyoplastra articulating weakly with the posterolateral portions of the entoplastron. Due to the curvature of the embryo, the hyo- and hypoplastra do not lie in one plane but are slightly angled relative to one another. The outlines of the hypo- and hyoplastra are similar in shape. Early ossification starts at the central-medial platy section and progresses medially and laterally. The hypoplastron then develops a more straight lateral process, whereas its main portion becomes larger. As observable in specimen 101 (Stage 24-), the central regions of the hyo- and hypoplastra still largely lack compact bone layers, thus the interior cancellous bone structures are visible. By stage 27, there are also two blunt lateral and four to five stronger and lesser medial pointed processes. The posterior protrusions of the hypoplastra interdigitate with the two most prominent anterior protrusions of the xiphiplastra. Each xiphiplastron develops as a tripartite structure with two prominent and few

additional small thin fingerlike anterior protrusions, two to three short medial protrusions, and a single massive posterior process. The anterior margin of the element is slightly concave and the medial margin is more strongly concave. During development, the lateral margin varies from being straight or concave to slightly convex in the posterior part of the xiphiplastron. As figured by Ogushi (1911:fig. 8), the posthatching shape of the lateral margin of the xiphiplastron is convex.

Ossification Patterns of the Appendicular Skeleton

Pectoral girdle (see Fig. 3). The pectoral girdle develops as a tripartite structure composed of the coracoid (posterior) and scapula [with a ventromedial process (i.e., the "acromion" process) and a dorsal process]. In the earliest stages examined, the pectoral girdle is mostly anterior to the cartilaginous anlage of the first rib. Only with the development, i.e., the ossification, of the nuchal bone and the anterior costal and neural bones of the carapace, does this girdle become enclosed within the shell. The coracoid forms the posterior portion of the the glenoid fossa, whereas the ventral margin of the lateral part of the scapula forms the anterior portion of this fossa. The coracoid and ventromedial process of the scapula lie on a horizontal plane subparallel to the plastron, and the dorsal process of the scapula is angled about 70° to the horizontal plane. The coracoid develops as a broad, blade-like element with a concave medial margin and a convex lateral margin. Posteriorly, the coracoid ends in a pointed cartilaginous tip that curves anteromedially ("epicoracoideum" of Ogushi, 1911: p. 71). The scapula develops as a straight cylinder. At its dorsal end, the scapula terminates in a posteriorly-bent cartilaginous process, described as the epiphysis of the scapula, the 'suprascapulare', and the 'os triquetrum Bojani' sensu Ogushi (1911: p. 71). The ventromedial process of the scapula is circular in cross section towards the glenoid fossa but medially it is dorsoventrally compressed. At its medial tip, the process is capped by a long prominent cartilaginous process that extends both anteriorly and posteriorly. Ogushi (1911: p. 71) interpreted wrongly the ventromedial process of the scapula as the clavicle, hence he named the medial cartilaginous process 'epiclaviculare'. Before the onset of ossification, the pectoral girdle appears as a continuous cartilaginous anlage without apparent demarcations. The scapula and its ventromedial process both start ossifying from separate centers at stage 23, whereas the coracoid starts to ossify at stage 24-. Ossification starts at the mid regions of the elements and progresses towards the glenoid fossa and the distal margins of each bone respectively. At stage 27, the adult morphology of the pectoral

girdle is already present, with only the distal tips of the bones retaining cartilage.

Forelimb (Figs. 5 and 6). The adult manus is composed of two proximal carpals (a larger ulnare and a smaller intermedium), one or two centralia, an elongate pisiform, Distal Carpals 1-5, Metacarpals I-V, and the phalanges; the phalangeal formula of the manus at hatching is 2-3-3-5-4 (see Fig. 5). The humerus first exhibits ossification at stage 20+, followed by the zeugopodial elements at stage 22. Because of individual variation among the specimens studied, there is no unambiguous ossification sequence during growth (see Fig. 6). However, the metacarpals and phalanges generally ossify before the proximal and distal carpals around stages 24 and 25. The distal carpals ossify earlier than the proximal carpals, and the second distal carpal is the first to ossify. Ossification of the pisiform coincides with the ossification of Distal Carpal 5. The ulnare ossifies before the intermedium. In several specimens from stage 27– onward, a second isolated central element starts ossifying.

Pelvic girdle (Figs. 3 and 4). Before the onset of ossification, the cartilaginous anlage of the three pelvic bones appears to be continuous. The shape of the pelvic girdle does not change much from pre-ossification stages to well ossified forms. In well ossified specimens (e.g., stage 27), cartilaginous symphyses are present between the pubes and ischia. The pubis and ischium lie in one horizontal plane, whereas the rod-like ilium extends dorsally and slightly posteriorly. In all specimens and stages studied, a large cartilaginous prepubis remains situated anterior to the pubic bones. Similarly, the posterodorsal tip of the ilium and the posterior tip of the ischium remain cartilaginous. As indicated by retention of Alizarin red, ossification of all three pelvic bones commences at stage 24–. Similar to the condition in the pectoral girdle, ossification starts at the mid-parts of the elements.

Hind limb (Figs. 5 and 6). The adult pes includes one large proximal tarsal, the astragalocalcaneum complex, and four distal tarsals, with the fourth being the largest (see Fig. 5). The recorded phalangeal formula of the pes at hatching is 2-3-3-4-3. The general scheme of ossification in the hind limb is generally similar to the one found in the forelimb. The ossification of the stylo- and zeugopodial elements in the hind limb coincide with those of the serial homologous structures in the forelimb, as the femur starts retaining Alizarin red at stage 20+, the tibia and fibula at stage 22. The first autopodial elements to ossify are the Metatarsals II-IV (stage 24) followed by the phalanges. Among the metatarsals, the fifth hooked metatarsal is the last to ossify. Only when ossification started in all phalanges, the onset of ossification was recorded in the distal tarsals. The proximal tarsal, i.e., the astragalocalcaneum, starts ossifying shortly after the first distal tarsals,

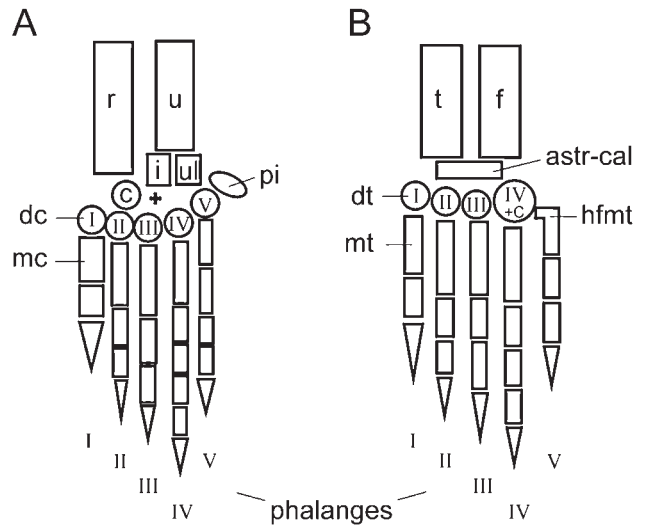


Fig. 5. Schematic representation of left zygopodial and autopodial elements (A, manus; B, pes) of adult *Pelodiscus sinensis*.

and is well ossified at stage 27. As in the manus, marked individual variation was recorded among the specimens (see Fig. 6).

Parsimov Analysis: General Results

The rank ordered ossification sequence for *Pelodiscus sinensis* studied by us comprises 66 ossification events, compared with data from the literature as cited above. These characters represent ossification events in the cranium (28 events), postcranial axial skeleton (17 events, including ribs, vertebrae, and plastral elements), pectoral girdle and forelimb (11 characters), and pelvic girdle and hind limb (10 characters). These ossification events were compared and summarized in a data matrix of event pairs, yielding a total of 2145 event pair comparisons. Of these, 351 (16.4%) represent comparisons of cranial vs. cranial elements, 1053 (49.1%) represent comparisons of cranial vs. postcranial elements, and 741 (34.5%) represent comparisons of postcranial vs. postcranial elements. Two Parsimov analyses were performed on the event pairs, one with the original data and a second with all event-pair ties converted from score "1" to score "?". The results are reported in tabular form and in the Supporting Information to this paper. The discussion of the Parsimov results are based on the consensus of ACCTRAN and DELTRAN optimizations on the phylogenetic framework of Figure 1.

Ossification Sequence Changes in the Main Clades Detected with Parsimov (see Fig. 1)

Hypothetical last common ancestor of cryptodire turtles examined: Seven elements were inferred to

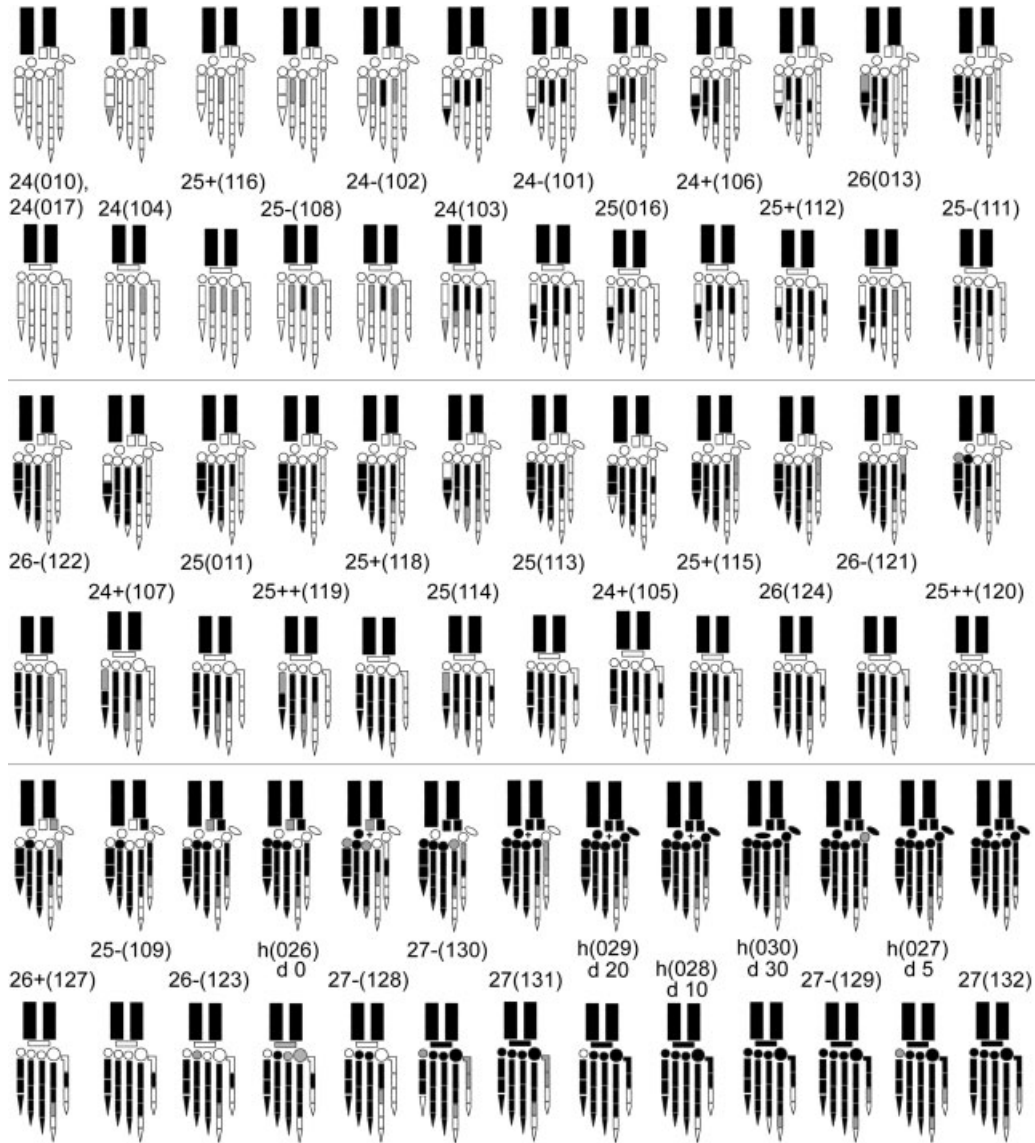


Fig. 6. Schematic diagram of the sequential ossification of the zygopodial and autopodial bones in *Pelodiscus sinensis*. Each cleared and double-stained specimen under study is indicated by its developmental stage, followed by the specimen number in parentheses. “Minus” (–) and “plus” symbols (+,++) indicate early and late examples of a respective stage. Hatchling specimens are marked with an “h” in front of the specimen number and the days after hatching (“d”) are given respectively. The onset of ossification for each element is based on the initial retention of Alizarin Red. Elements shown in white are still cartilaginous, weak initial ossification is marked by gray color, and well ossified elements are in marked in black color. The occurrence of a second central element in the manus of some specimens of *P. sinensis* is indicated by a “plus” symbol (+). Note that in specimen (112), stage 25, the left manus and pes are only weakly stained, whereas the right elements show overall good staining results. Please refer to Figure 5 for the identity of the structures represented.

shift earlier in development relative to other elements. Of these, four (maxilla, prefrontal, parietal, and squamosal) are dermal bones of the cranium that shifted early relative to other dermal elements of the cranium, or to elements of the fore- and hind limb. In the maxillary arcade of the skull, the maxilla shifted earlier relative to two dermal bones of the lower jaw (dentary and surangular). The prefrontal, parietal, and squamosal (dermal bones of the skull table and temporal

region) were inferred to shift earlier relative to the jugal (which plays a functional role between the maxilla and palatal series), and the temporal elements of the dermal roofing series (Rieppel, 1980), as an element that forms part of the suspensorium and temporal region. Only one group of elements (metatarsals) were inferred to shift later in development relative to the quadratojugals. In the postcranial axial skeleton, the thoracic centra shifted early relative to those of the cervical region.

Neural arches of the caudal and sacral vertebrae also shifted earlier relative to elements of the fore- and hind limb.

Trionychidae. Seven elements were inferred to change their relative position in the sequence of ossification. Four elements (surangular, quadrate, epiplastron, and thoracic centra) were found to move earlier, whereas three (premaxilla, caudal, and sacral centra) were found to move relatively later. The surangular (a dermal bone of the lower jaw) and the thoracic centra shifted earlier in position relative to the zeugopodial elements in both the fore- and hind limb. The quadrate shifted earlier relative to girdle elements of the forelimb (scapula and acromion) and hind limb (ilium), as well as the distal elements of the forelimb (phalanges of manus). No shifts were identified in the timing of ossification of the quadrate relative to any dermal elements, however, the quadrate was observed to ossify relatively earlier than the exoccipital. The only late-shift of any dermal element of the skull was the premaxilla (an element of the maxillary arcade) relative to the jugal and frontal (elements of the temporal region and skull roof, respectively).

Pelodiscus. Nine elements were inferred to alter position in the sequence of ossification. The prefrontal, squamosal, pterygoid, and surangular (dermal bones of the skull table, temporal region, palatal series, and lower jaw, respectively) shifted to later positions relative to the hyoplastra, hypoplastra, and xiphoplastra and thoracic centra; the pterygoid shifted to a position later than the stylo-podial elements of both the forelimb and hind limb. Several endochondral elements of the skull shifted to earlier positions relative to elements of the skull, limbs, and postcranial axial skeleton. In particular, the basisphenoid and columella both shifted earlier than the prearticular and quadratojugal, whereas the columella also shifted earlier than the premaxilla, vomer, and exoccipital, proximal elements of the pectoral and pelvic girdles (scapula, acromion, and ilium), and elements associated with the vertebral column (costals, caudal and sacral centra, and cervical neural arches). The cervical vertebrae shifted early relative to several dermal bones of the skull (coronoid, parietal, jugal, angular, prearticular, quadratojugal) and the stylo- and zeugopodial elements of the forelimb and hind limb. The sacral neural arches shifted late relative to the opisthotic (endochondral bone of the posterior half of the otic capsule) and ischium.

Chondrocranium of *Pelodiscus sinensis* at Stage 20 (see Fig. 7)

The chondrocranium is dominated by cartilages of the braincase and orbital region, and in general the nasal capsules and anterior chondrocranium are gracile and lightly built. As seen in lateral

view (see Fig. 7), the anterior half of the chondrocranium is directed ventrally. The major differences with other turtles can be observed in the anterior portion of the orbitotemporal region, particularly where it interacts with the nasal capsules.

Nasal capsules. The nasal capsules occupy the anterior one-fourth of the chondrocranium and are curved strongly ventrally relative to the long axis of the cranium. The nasal septum extends posteriorly only slightly beyond the level of the planum antorbitale and does not extend anteriorly to the margins of the fenestrae narina. The parietotectal cartilage is convex and extends laterally from the nasal septum to form the roof of each nasal capsule. As seen in dorsal and lateral views the foramen epiphaniale pierces the posterodorsolateral region of the parietotectal cartilage, slightly anterior to the level of the planum antorbitale; based on examination of all available specimens, the posterior margin of the foramen epiphaniale is incomplete. As in *Emys orbicularis* (Bellairs and Kamal, 1981:208), the lateral branch of the ethmoidal nerve is inferred to exit the foramen epiphaniale, but the precise route taken by this nerve is unclear as the relative degree of chondrification in this region is low, and the arrangement of several cartilages differs from that observed in other turtles. The ectochoanal cartilages extend posteriorly only slightly beyond the margins of the planum antorbitale. The fenestra narina are relatively wide and conspicuous at the snout, and the walls are thin and weakly stained. Each planum antorbitale bears a thin, conspicuous plate of cartilage that is positioned horizontal to the long axis of the chondrocranium and extends posteriorly nearly to the level of the anterior margin of the planum suprasedptale. Cartilages such as these have been interpreted as the maxillary processes of the paranasal cartilages. As seen in ventral view, the lamina transversalis anterior is longer than wide and slightly concave. Prominent canals for the anterior nasal vessels lie parallel to the nasal septum and are bordered laterally by the paraseptal cartilages; the foramen prepalatinum lies at the anterior extent of each canal. The internal choanae are relatively large and directed posteriorly.

A noteworthy aspect of the chondrocranium is the lack of contact between the nasal capsules and planum suprasedptale via the sphenethmoid commissurae. As seen in dorsal and lateral views, thin, triangular sphenethmoid commissurae are present but each is completely independent of the nasal septum (which remains an unbranched, median cartilage) and the plana suprasedptale (which diverge slightly at their anterior termini). The sphenethmoid commissurae lie vertically relative to the horizontal plane of the chondrocranium and are positioned between the posterior terminus of the nasal septum and the anterior margins of the plana suprasedptale; the sphenethmoid commis-

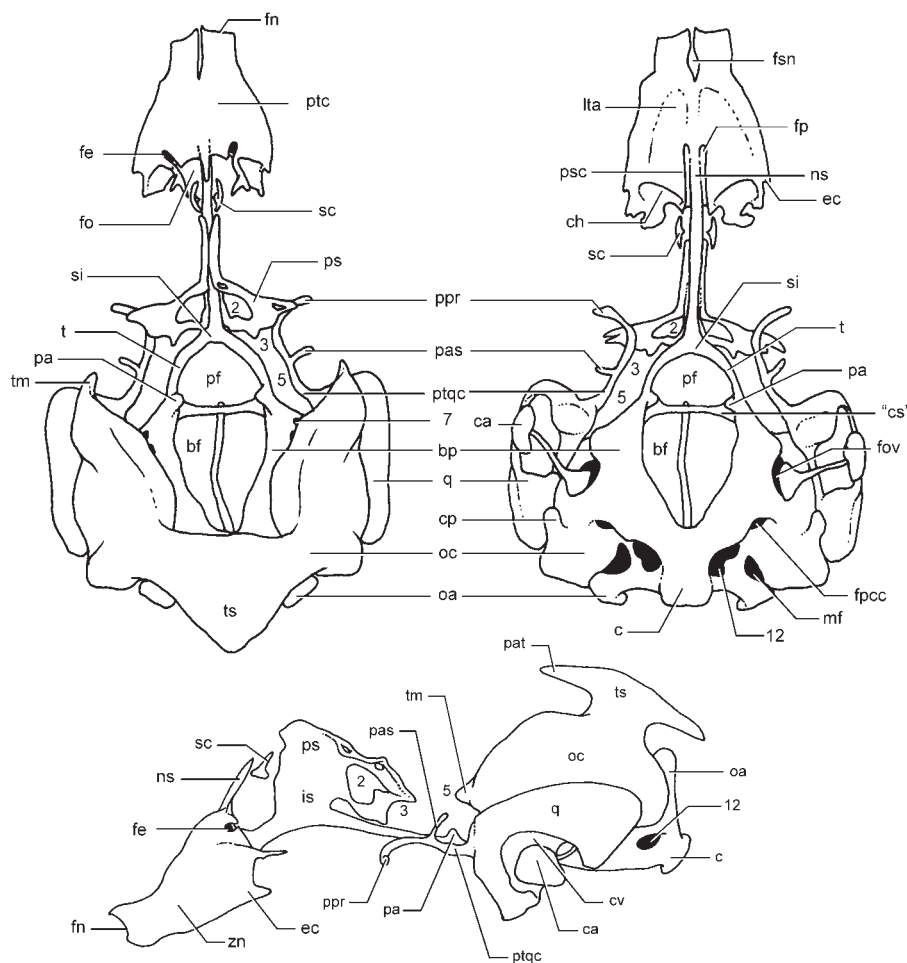


Fig. 7. Chondrocranium of TK stage 20 in *Pelodiscus sinensis* in dorsal (left), ventral (right) and lateral view (below). Numbers and abbreviations used are: 2, optic fenestra; 3, foramen for oculomotor nerve; 5, prootic fenestra (for foramen nervi trigemini); 7, foramen for facial nerve; 8, foramen nervi abducentis; 12, foramina for hypoglossal nerves (i.e. foramen nervi hypoglossi of adults); bf, basicranial fenestra; bp, basal plate; c, occipital condyle (i.e. condylus occipitalis of adults); ca, columella auris; ch, choanal opening (i.e. apertura narium externa of adults); cp, crista parotica; cs, crista sellaris; cv, cavum tympani; ec, ectochoanal cartilage; fe, foramen epiphaniale; fn, fenestra narina (i.e. apertura narium interna of adults); fo, fenestra olfactoria; foa, foramen for ophthalmic artery; fov, fenestra ovalis; fp, foramen prepalatinum; fsn, fenestra septi nasi; is, interorbital septum; lta, lamina transversalis anterior; mf, metotic fissure; n, notochord swelling; ns, nasal septum; oa, occipital arch; oc, otic capsule; onf, orbitonasal fissure; pa, pila antotica; pas, anterior process of palatoquadrate cartilage; pat, anterior process of tectum synoticum; pf, pituitary fenestra; pla, planum antorbitale; pm, pila metoptica; ppr, pterygoid process of palatoquadrate cartilage; ps, planum suprasedale; psc, parasagittal cartilage; ptc, parietotectal cartilage of zona annularis; ptqc, palatoquadrate cartilage; q, quadrate cartilage; rc, rostral cartilage; sc, sphenethmoid commissure; si, subiculum infundibuli; t, trabecula communis; tm, taenia marginalis; ts, tectum synoticum; zn, zona annularis. Not to scale.

surae were not observed to contact either of these structures in any available specimens. As seen in dorsal view, the fenestra olfactoria advehens (defined by the margins of the parietotectal cartilage, nasal septum, and sphenethmoid commissurae) is relatively broad. However, given that the observed positions of the sphenethmoid commissurae and the dorsal projection of the nasal septum, it is assumed that the margins of the fenestra olfactoria advehens are slightly different than those observed in other turtles, and that the route of the olfactory and vomeronasal nerves may differ slightly in *P. sinensis*. Restructuring of this entire

region is quite apparent. Major modifications are observed in the slender posterodorsally-directed nasal septum, reduced and isolated sphenethmoid commissurae, and deeply-inscribed anterior margin of the interorbital septum and planum suprasedale (which are not continuous with the nasal septum), all of this leading to an orbitonasal fissure that is large and open in all available specimens, and the sphenethmoid commissurae are never observed to unite the nasal capsules plana suprasedale.

Quadrate cartilages and otic capsules. The quadrate cartilages are approximately half the size

of the otic capsules and bear slender palatoquadrate cartilages that possess thin ascending and anterior processes. The anterior process of the palatoquadrate cartilage extends beyond the lateral-most margins of the planum suprasedale (likely due to reduction of the cartilages of the planum suprasedale). The main body of the quadrate cartilage is twice as long as the palatoquadrate cartilage, and in general the corpus is twice as long as high; the cavum tympanicum occupies less than half of the lateral wall of the quadrate. The area articularis is prominent and extends well below the ventral margin of the basal plate of the braincase. The otic capsules are relatively large and robust and by later stages of development exhibit strong chondral fusion with the lateral margins of the basal plate. The medial wall of each otic capsule is pierced by the foramen for the facial nerve, paired foramina for auditory nerves, foramen for the glossopharyngeal nerve, and foramen for the endolymphatic duct. Prominent, knob-like crista parotica are present on the posteroventrolateral margin of each otic capsule; each extends slightly below the posterior terminus of the quadrate cartilage. The tectum synoticum is broad and thin, with prominent anterior and posterior processes. The taenia marginalis is a thin and triangular process that extends from the anterior margin of each capsule.

Basal plate and occipital region. The parachordal cartilages are separated medially by a prominent basicranial fenestra that is nearly twice as long as wide. The anterior extent of the basal plates is marked by the presence of extremely reduced pila antotica that are as high as wide. The occipital region bears general similarities to the adult cranium in terms of passage for vessels and nerves. The foramen posterius canalis carotici is relatively large and positioned anteromedial to the crista parotica, whereas posteromedial to this foramen are the anatomical spaces for the cavum internum, foramen jugulare laterale, foramen jugulare externum, and fenestra perilymphaticum. At stage 21, a single, relatively large foramen nervi hypoglossi is present anterior to the base of the occipital arch, and accommodates the passage of the hypoglossal nerve; these structures are paired in adults.

Orbitotemporal region. The interorbital septum is higher than long and, as seen in lateral view, occupies approximately one-fifth of the length of the chondrocranium. The interorbital septum is reduced along the anterior margin, leaving space for a large orbitonasal fissure. Each planum suprasedale is reduced in form and, as seen in dorsal view, these paired structures diverge only slightly. The anterior margin of the planum suprasedale and interorbital septum do not contact the sphenethmoid commissurae or the interorbital septum. At the level of the anterior margin of the optic fenestra, the posterior half of each pla-

num suprasedale is directed perpendicular to the midline axis of the chondrocranium; each extends laterally nearly to the level of the lateral terminus of the anterior processes of the palatoquadrate cartilages. The pila metoptica are absent and the posteroventral margin of the foramen for the ophthalmic artery is open posteriorly; therefore, the posteroventral margin of each planum suprasedale is deeply inscribed. Several cartilages typically associated with formation of the pila metoptica (anteroinferior process, posteroinferior process, supratrabecular cartilage) are presumed either to be absent or to occupy radically different positions in the posterior portion of the orbitotemporal region. A detailed study of the anatomical positions for the origin of the eye musculature in *P. sinensis* will be required to elucidate precisely the modifications of cartilages observed in this region. In early-stage specimens (e.g., stage-17, Specimen 024), the posterior orbital cartilage presents a typical morphology and position at the anterior terminus of the notochord; however, by stage 21 this cartilage is greatly reduced at midbody and only a tiny, knob-like pila antotica projects dorsomedially at the level of interaction between the trabeculae and basal plates. The resulting anatomy (and lack of chondrification of the ventral portion of the posterior orbital cartilage) is such that the crista sellaris appears to be absent in *P. sinensis*. Despite lack of chondrification in this region, nonstaining connective tissue does persist in this region to separate the pituitary and basicranial fenestrae. Though this region does not appear to chondrify in any of the available specimens, adults of this species do possess a prominent dorsum sellae and processus clinoides (Ogushi, 1911; personal observation), which are known to form by endochondral ossification of the crista sellaris and pila antotica, respectively.

Chondrogenesis in the Forelimb and the Hind Limb

Although limited, the data are sufficient to record the gradual proximodistal (in early specimens) and preaxial-postaxial (in older specimens) appearance of the anlage of autopodial structures (see Fig. 8). The series documents an increase of the phalangeal formula. Because of lack of resolution, nothing can be reported on the connectivity among elements (Shubin and Alberch, 1986), so we restrict ourselves to the identification of elements appearing on subsequent stages.

Forelimb. The earliest stage of chondrogenesis observed includes the anlagen of the radius and the ulna; distal to the latter are the anlagen of ulnare and Distal Carpal 4, forming the beginning of the primary axis. Also present are anlagen for the intermedium and for all digits except the fifth one. The following stage is much more advanced, exhibiting anlagen of the five digits, four distal carpals

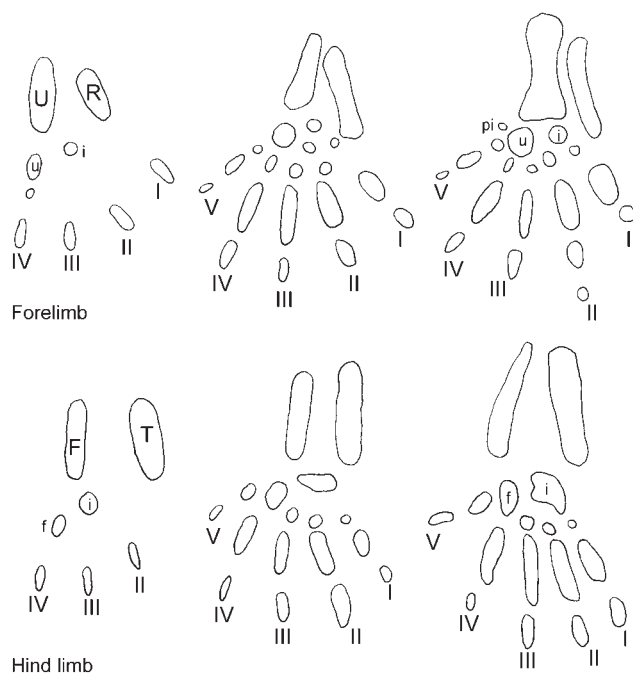


Fig. 8. Chondrification sequence of the right forelimb (top) and hind limb (bottom) in *Pelodiscus sinensis* in dorsal view, documented with camera lucida drawings. Not to scale. The sequence of specimens is from left to right: stages 16, 17, and 18; numbers refer to Tokita and Kuratani (2001) stages. Abbreviations refer to anlage of several elements and include: c, centrale; F, fibula; f, fibulare; i, intermedium; pi, pisiform; T, tibia. The roman numerals refer to the digits. Not to scale.

and two middle carpal condensations most likely representing the anlage of two centralia or one centrale and Distal Carpal 1 in a location much more proximal than expected. One of these two anlagen is absent in the next stage, which presents all five distal carpals and the pisiform. This may be the result of fusion of elements or of individual variation.

Hind limb. The youngest specimen examined shows the anlagen for the tibia, fibula, fibulare, and Distal Tarsal 4, exhibiting the primary axis as well as the anlage for structures related to Digits II and III. The next stage exhibits anlagen of elements of all five toes; here five distal tarsals and a large proximal tarsal element are recognized. The third stage illustrated here has the same number of elements; only the shape and relative size of them is different.

DISCUSSION

Heterochrony and Variation in Skeletal Development

Patterns of ossification of cranial dermal elements are generally more variable than are those of endochondral elements of the braincase, and dermal elements ossify before endochondral elements. Compared to *Apalone spinifera*, the only

other trionychid for which extensive data on the development of the skull are available (Sheil, 2003), most ossifications develop later in *P. sinensis*. Differences in ossification sequences between the two species are also present in: *P. sinensis* the jugal develops relatively early and before the frontal, whereas it appears later in *A. spinifera*; the frontal appears shortly before the parietal in *A. spinifera*, whereas in *P. sinensis* the parietal appears several stages before the frontal. As expected, both soft-shelled turtles are more similar to each other in ossification sequence than the two chelydrid turtles *Chelydra serpentina* (Sheil and Greenbaum, 2005) and *Macrochelys temminckii* (Sheil, 2005). Both chelydrids show an early development of the postorbital bone and the palatal elements as compared to the trionychids investigated.

A quantitative comparison of the amount of sequence heterochrony in the cryptodire turtle data set presented here with those in recent comprehensive studies of mammals (Sánchez-Villagra et al., 2008a; Weisbecker et al., 2008) or vertebrates in general (Schoch, 2006) is not possible at present. The sampling for turtles is much restricted and also the turtle data set integrates in the same analysis cranial and postcranial data, which are treated separately in the previous comprehensive studies. However, a comparison of the average number of heterochronic changes as measured by the consensus of ACCTAN and DELTRAN changes at all internal nodes of the tree reveals that this number is larger in turtles than in mammals (Sánchez-Villagra et al., 2008a; Weisbecker et al., 2008), suggesting that heterochrony in ossification sequences in turtles is more prevalent.

As described for *Chelydra serpentina* (Sheil and Greenbaum, 2005), much plasticity in ossification within autopodials is observed. However, some general patterns were recorded. The three middle metacarpals are the first elements in the manus to start ossification (although Distal Carpal 1 starts earlier in one specimen), as in *Apalone spinifera* (Sheil, 2003) and *Chelonia mydas* (Sánchez-Villagra et al., 2007). In *Trachemys scripta* (Sheil and Portik, 2008) a similar pattern is present. Which carpal element is the first to start ossification is quite variable among cryptodire turtles. The published information is as follows: *Caretta caretta* and likely *Chelonia mydas*, ulnare and radiale (Sánchez-Villagra et al., 2007); *Kinosternon* sp., Distal Carpal 4 (Rieppel, 1993a); *Apalone spinifera*, Distal Carpals 14 (Sheil, 2003); and *Chelydra serpentina*, Distal Carpals 1-2 (Sheil and Greenbaum, 2005). The pattern of ossification of tarsal elements described herein is broadly consistent with that reported for other turtles (Sheil and Portik, 2008). In *P. sinensis* distal tarsals are the first to commence ossification, followed by the proximal compound element.

The significance (functional or otherwise) of many of the heterochronic changes detected by

Parsimov is unclear. For example, in *P. sinensis*, the metatarsals were inferred to shift later in development relative to the quadratojugals. Event pairing in a comprehensive analysis such as the one presented here, creates pairs of events which are connected in no biologically significant way other than the order of comparisons made through the event-pair matrix. Once enough empirical data are available for turtles, this study could be expanded into an examination of heterochrony in developmental modules, identified via Parsimov (Jeffery et al., 2005; Ziermann, 2008) or via another recently developed method (Harrison and Larsson, 2008).

Bever (2008, 2009; see also Maisano, 2002; Joyce and Bell, 2004) has conducted studies of postnatal ontogeny in turtle skulls that have emphasized some of the significant changes that occur in characters that are commonly used in phylogenetic analyses. He emphasized the necessity for studies of variation to understand its phylogenetic distribution and modularity. Bever (2009: p. 97) stated, "the available empirical data lag seriously behind recent theoretical advances that broaden the application of intraspecific variation data for discrete characters to phylogenetic and evolutionary questions." This statement is also true for studies of skeletal development such as the one presented here. The rare possibility to examine a large number of specimens revealed much variation in the sequence within some areas such as autopodial elements. However, we do not think that this variation has affected the overall analysis of heterochrony, as many of these elements were lumped into modules or structural units (e.g., metacarpals, metatarsals, phalanges of manus, phalanges of pes), which as such have a typical timing pattern of ossification onset in the skeleton. If examination of heterochrony within autopods were to be a subject of study, we would first need much more information on other turtle species. Only then could an application of recent methodological developments that deals with such variation in studies of sequence heterochrony be warranted (Colbert and Rowe, 2008).

Morphological Patterns and Shell Ontogeny

Examination of this developmental series has allowed us to observe and document the changing relations of the pectoral girdle with the developing carapace. Figuring out the nature of the topographical relation of this girdle with the shell has been a central point in studies of the origin of the turtle body plan (Burke, 1989; Gilbert et al., 2001; Nagashima et al., 2007). We confirm that only with the development of the complex anterior portion of the carapace resulting from metaplastic ossification (Scheyer et al., 2008), does the pectoral girdle become enclosed in the shell (Lyson and Joyce, 2008).

Our observations of the developing nuchal and plastral bones in *Pelodiscus sinensis* are comparable with the conditions in *Trachemys scripta* and *Chelydra serpentina* (e.g., Gilbert et al., 2001), in that these elements develop through a primary and secondary phase of ossification. Basically, the primary phase of ossification starts with the appearance of the unstained rod-like structures at stage 18 and 19. Based on limited sampling of older hatchling specimens, however, the second phase that finally leads to the plate-like formation of the bones in adult specimens of *P. sinensis* (see Ogushi, 1911: plate 2, Figs. 8 and 9), is not recorded in our developmental series. In comparison to the nontrionychid species, the primary deeper bar- or rod-like structures are not fully incorporated into the secondary, more superficial plate-like parts, so that their primary outlines are largely traceable throughout ontogeny in *P. sinensis*. The primary and secondary phases of ossifications are both part of the primary, thecal shell. We confirm Cherepanov's (1995) observations that there are no isolated epithelial (sensu Zangerl 1969) trionychid shell during development.

In trionychids, the neural series is highly variable concerning the shape and number of elements (e.g., Gardner and Russell, 1994). Ogushi (1911) mentioned only seven neurals in *Pelodiscus sinensis* however an additional neural separating the anterior part of the eighth (= posterior-most) pair of costals can be present. Furthermore, due to the presence of a preneural in some specimens, a plate that can occur directly posterior to the nuchal bone, Meylan (1987) considered the preneural to be the neural 1, thus reporting eight neurals instead of seven in ten individuals and nine neurals instead of eight in 15 individuals of *P. sinensis*. Accordingly, in those specimens with lower neural numbers, the preneural (or neural 1) and the adjacent posterior neural (or neural 2) would have been fused. Cherepanov (1995), on the other hand, expressed that the contact between the preneural plate and the first dorsal vertebra is sutural (= secondary), and thus that the preneural cannot be a neural in the strict sense. The stage 27 specimens in the developmental series studied herein show only ossification of the neural arches but no neural plate development so far. Our series thus does not allow addressing this circumstance further, because of the lack of older hatchling specimens. At no point during development, anlagen of peripheral, pygal, or suprapygal bones were present in *Pelodiscus sinensis*, further confirming the absence of these bones in Trionychidae.

The Limb Chondrification Pattern

In a series of articles, Rieppel (e.g., 1992; 1993a,b) documented and indicated that chondrification and ossification are decoupled phenomena,

confirming this previous observation by de Beer (1937) and by later workers including ourselves (Sheil, 2005; Sánchez-Villagra et al., 2007). Data presented here for *P. sinensis* confirms this pattern. In the limb of *Pelodiscus*, the departure from the primary axis and digital arch patterns of chondrogenesis in the ossification sequence is more marked than is generally seen across tetrapods (Fröbisch, 2008).

Although the data available to us on chondrogenesis are limited, they are in accordance with the existence of a primary axis and digital arch. We find no evidence of anterior condensations distal to the radius and the tibia, respectively, suggesting that the radiale and tibiale are absent, as in other turtles examined to date (Burke and Alberch, 1985; Sánchez-Villagra et al., 2007; Sheil and Portik, 2008; Fabrezi et al., 2009).

The second specimen of the *Pelodiscus sinensis* forelimb in the series shown here (see Fig. 7) exhibits an element which, because of its position, is best homologized with the anlage of a centrale. A centrale is missing in the following stage as well as in the adult (Ogushi, 1911). This can be best explained with a reabsorption during development, although a fusion with other elements (we did not find traces of this) or individual variation in the presence of centralia cannot be ruled out. In this context, it is worth pointing out that there is no apparent connectivity between or among any centralia and other autopodial elements in several turtle species treated by several other authors (Burke and Alberch, 1985; Sheil and Portik, 2008; Sánchez-Villagra et al., 2008b). This lack of connectivity may explain the higher degree of variation recorded in the development of the centralia region of the autopod.

In their study of relative sequence of 10 events in the early development of the forelimbs versus the hind limbs in 14 tetrapod species spanning a diverse taxonomic, ecomorphological and life-history range, Bininda-Emonds et al. (2007) found a rather simultaneous development of the two in most tetrapods, including the turtle *Emys orbicularis*. This pattern of quasi-simultaneity is seen in the chondrogenesis of all turtles examined to date (e.g., Sánchez-Villagra et al., 2008b) and is recorded here also for *Pelodiscus sinensis*. However, the identification of patterns of forelimb-hind limb heterochrony may be critically sensitive to the characters studied, i. e., different aspects of limb development may show different forelimb-hind limb timing relations (Richardson et al., in press).

ACKNOWLEDGMENTS

The visit of MRSV to Kobe was made possible by the RIKEN Center for Developmental Biology. The authors thank Christian Mitgutsch, Ingmar

Werneburg, Janine Ziermann, and Olaf Bininda-Emonds for discussions on sequence heterochrony and Parsimov, and Gabe Bever (AMNH; New York) and an anonymous reviewer for careful and useful reviews that helped to improve the manuscript.

LITERATURE CITED

- Bellairs A d'A, Kamal AM. 1981. The chondrocranium and the development of the skull in recent reptiles. In: Gans C, Parsons TS, editors. *Biology of the Reptilia*, Vol. 11: Morphology. London: Academic Press. pp 1–263.
- Bever GS. 2008. Comparative growth in the postnatal skull of the extant North American turtle *Pseudemys texana* (Testudinoidea: Emydidae). *Acta Zool (Stockholm)* 89:107–131.
- Bever GS. 2009. The postnatal skull of the extant North American turtle *Pseudemys texana* (Cryptodira: Emydidae), with comments on the study of discrete intraspecific variation. *J Morphol* 270:97–128.
- Bickham JW, Iverson JB, Parham JF, Philippen H-D, Rhodin AGJ, Shaffer HB, Spinks PQ, van Dijk PP. 2007. An annotated list of modern turtle terminal taxa with comments on areas of taxonomic instability and recent change. *Chelonian Res Monogr* 4:173–199.
- Bininda-Emonds ORP, Jeffery JE, Sánchez-Villagra MR, Hanken J, Colbert M, Pieau C, Selwood L, Cate CT, Raynaud A, Osabutey CK, Richardson MK. 2007. Forelimb-hind limb developmental timing across tetrapods. *BMC Evol Biol* 7:182.
- Bona P, Alcalde L. 2009. Chondrocranium and skeletal development of *Phrynosoma hilarii* (Pleurodira: Chelidae). *Acta Zool (Stockholm)* 90: doi: 10.1111/j.1463-6395.2008.00356.x.
- Burke AC. 1989. Development of the turtle carapace: Implications for the evolution of a novel bauplan. *J Morphol* 199:363–378.
- Burke AC, Alberch P. 1985. The development and homology of the chelonian carpus. *J Morphol* 186:119–131.
- Cherepanov GO. 1995. Ontogenetic development of the shell in *Trionyx sinensis* (Trionychidae, Testudinata) and some questions on the nomenclature of bony plates. *Russian J Herpetol* 2:129–133.
- Colbert MW, Rowe T. 2008. Ontogenetic sequence analysis: Using parsimony to characterize developmental sequences and sequence polymorphism. *J Exp Zool B Mol Dev Evol* 310B:398–416.
- de Beer GR. 1937. *The Development of the Vertebrate Skull*. Oxford: Oxford University Press.
- Dalrymple GH. 1979. Packaging problems of head retraction in trionychid turtles. *Copeia* 1979:655–660.
- Engstrom TN, Shaffer HB, McCord WP. 2004. Multiple data sets, high homoplasy, and the phylogeny of softshell turtles (Testudines: Trionychidae). *Syst Biol* 53:693–710.
- Fabrezi M, Manzano A, Abdala V, Zaher H. 2009. Developmental basis of limb homology in pleurodiran turtles and the identity of the hooked element in the chelonian tarsus. *Zool J Linn Soc* 155:845–866.
- Fritz U, Havaš P. 2007. Checklist of chelonians of the world. *Vertebrate Zool* 57:149–368.
- Fröbisch NB. 2008. Ossification patterns in the tetrapod limb—Conservation and divergence from morphogenetic events. *Biol Rev* 83:571–600.
- Gaffney ES. 1990. The comparative osteology of the Triassic turtle *Proganochelys*. *Bull Amer Mus Nat Hist* 194:1–263.
- Gardner JD, Russell AP. 1994. Carapacial variation among soft-shelled turtles (Testudines: Trionychidae) and its relevance to taxonomic and systematic studies of fossil taxa. *N Jb Geol Palaeont Abh* 193:209–244.
- Gilbert SF, Loredó GA, Brukman A, Burke AC. 2001. Morphogenesis of the turtle shell: The development of a novel structure in tetrapod evolution. *Evol Dev* 3:47–58.
- Ginsberg J. 2002. CITES at 30, or 40. *Conserv Biol* 16:1184–1191.

- Harrison L, Larsson H. 2008. Estimating evolution of temporal sequence changes: A practical approach to inferring ancestral developmental sequences and sequence heterochrony. *Sys Biol* 57:378–387.
- Hedges SB, Poling LL. 1999. A molecular phylogeny of reptiles. *Science* 283:998–1001.
- Hill RV. 2005. Integration of morphological data sets for phylogenetic analysis of Amniota: The importance of integumentary characters and increased taxonomic sampling. *Syst Biol* 54:530–547.
- Jeffery JE, Bininda-Emonds ORP, Coates MI, Richardson MK. 2005. A new technique for identifying sequence heterochrony. *Syst Biol* 54:230–240.
- Jiang Zhi J, Castoe TA, Austin CC, Burbrink FT, Herron MD, McGuire JA, Parkinson CA, Pollock DD. 2007. Comparative mitochondrial genomics of snakes: Extraordinary rate dynamics and functionality of the duplicate control region. *BMC Evol Biol* 7:123.
- Joyce WG, Bell CJ. 2004. A review of the comparative morphology of extant testudinoid turtles (Reptilia: Testudines). *Asiatic Herp Res* 10:53–109.
- Kuraku S, Usuda R, Kuratani S. 2005. Comprehensive survey of carapacial ridge-specific genes in turtle implies co-option of some regulatory genes in carapace evolution. *Evol Dev* 7:3–17.
- Li C, Wu X-C, Rieppel O, Wang L-T, Zhao L-J. 2008. An ancestral turtle from the Late Triassic of southwestern China. *Nature* 456:497–501.
- Lyson T, Joyce WG. 2008. How did the turtle get its shoulder girdle inside its ribcage, or did it? *J Vertebr Paleontol* 28(Suppl. 3):109A.
- Maddison WP, Maddison DR. 2006. Mesquite: A modular system for evolutionary analysis. Version 1.12. Available at <http://mesquiteproject.org>.
- Maisano JA. 2002. The potential utility of postnatal skeletal developmental patterns in squamate phylogenetics. *Zool J Linn Soc* 136:277–313.
- Maxwell EE, Harrison LB. 2008. Ossification sequence of the common tern (*Sterna hirundo*) and its implications for the interrelationships of the Lari (Aves Charadriiformes). *J Morphol* 269:1056–1072.
- Meyer A, Zardoya R. 2003. Recent advances in the (molecular) phylogeny of vertebrates. *Ann Rev Ecol Evol Syst* 34:311–338.
- Meylan PA. 1987. The phylogenetic relationships of soft-shelled turtles (Family Trionychidae). *Bull Amer Mus Nat Hist* 186:1–101.
- Ministry of Agriculture, Forestry and Fisheries of Japan. 2007. The 2005 statistical report on fishery and cultivation industry production. Tokyo: The Incorporated Foundation of Agriculture and Forestry Statistics (in Japanese).
- Müller J. 2003. Early loss and multiple return of the lower temporal arcade in diapsid reptiles. *Naturwissenschaften* 90: 473–476.
- Nagashima H, Kuraku S, Uchida K, Ohya YK, Narita Y, Kuratani S. 2007. On the carapacial ridge in turtle embryos: Its developmental origin, function and the chelonian body plan. *Development* 134:2219–2226.
- Nagashima H, Uchida K, Yamamoto K, Kuraku S, Usuda R, Kuratani S. 2005. Turtle-chicken chimera: An experimental approach to understanding evolutionary innovation in the turtle. *Dev Dyn* 232:149–161.
- Nakane Y, Tsudzuki M. 1999. Development of the skeleton in Japanese quail embryos. *Dev Growth Differ* 41:523–534.
- Ogushi K. 1911. Anatomische Studien and der japanischen dreikralligen Lippenschildkröte (*Trionyx japonicus*). *Morph Jahrb* 43:1–106.
- Ohya YK, Kuraku S, Kuratani S. 2005. Hox code in embryos of Chinese soft-shelled turtle *Pelodiscus sinensis* correlates with the evolutionary innovation in the turtle. *J Exp Zool B Mol Dev Evol* 304B:107–118.
- Reisz RR, Head JJ. 2008. Palaeontology: Turtle origins out to sea. *Nature* 456:450–451.
- Richardson MK, Chipman AD. 2003. Developmental constraints in a comparative framework: A test case using variations in phalanx number during amniote evolution. *J Exp Zool B Mol Dev Evol* 296B:8–22.
- Richardson MK, Gobes S, Leeuwen A van, Poelman A, Pieau C, Sánchez-Villagra MR. 2009. Heterochrony in limb evolution: Developmental mechanisms and natural selection. *J Exp Zool B Mol Dev Evol* 312B: DOI: 10.1002/jez.b.21250.
- Rieppel O. 1980. The skull of the upper Jurassic cryptodire turtle *Thalassemys*, with a reconsideration of the chelonian braincase. *Palaeontographica Abt A* 171:105–140.
- Rieppel O. 1992. Studies on the skeleton formation in Reptiles. III. Patterns of ossification in the skeleton of *Lacerta vivipara* Jaquin (Reptilia, Squamata). *Fieldiana Zool* 68:1–25.
- Rieppel O. 1993a. Studies on skeleton formation in reptiles: Patterns of ossification in the skeleton of *Chelydra serpentina* (Reptilia, Testudines). *J Zool* 231:487–509.
- Rieppel O. 1993b. Studies on skeleton formation in reptiles. V. Patterns of ossification in the skeleton of *Alligator mississippiensis* Daudin (Reptilia, Crocodylia). *Zool J Linn Soc* 109: 301–325.
- Rieppel O. 1995. Studies on skeleton formation in reptiles: Implications for turtle relationships. *Zoology* 98:298–308.
- Rieppel O. 2004. Kontroversen innerhalb der Tetrapoda—Die Stellung der Schildkröten (Testudines). *Sitzungsberichte der Gesellschaft Naturforschender Freunde zu Berlin* 43:201–221.
- Rieppel O, deBraga M. 1996. Turtles as diapsid reptiles. *Nature* 384:453–455.
- Sánchez-Villagra MR. 2002. Comparative patterns of postcranial ontogeny in therian mammals: An analysis of relative timing of ossification events. *J Exp Zool B Mol Dev Evol* 294:264–273.
- Sánchez-Villagra MR, Mitgutsch C, Nagashima H, Kuratani S. 2007. Autopodial development in the sea turtles *Chelonia mydas* and *Caretta caretta*. *Zool Sci* 24:257–263.
- Sánchez-Villagra MR, Goswami A, Weisbecker V, Mock O, Kuratani S. 2008a. Conserved relative timing of cranial ossification patterns in early mammalian evolution. *Evol Dev* 10: 519–530.
- Sánchez-Villagra MR, Ziermann JM, Olsson L. 2008b. Limb chondrogenesis in *Graptemys nigrinoda* (Emydidae), with comments on the primary axis and the digital arch in turtles. *Amphibia-Reptilia* 29:85–92.
- Scheyer TM, Sander PM, Joyce WG, Böhme W, Witzel U. 2007. A plywood structure in the shell of fossil and living soft-shelled turtles (Trionychidae) and its evolutionary implications. *Org Div Evol* 7:136–144.
- Scheyer TM, Brüllmann B, Sánchez-Villagra MR. 2008. The ontogeny of the shell in side-necked turtles, with emphasis on the homologies of costal and neural bones. *J Morphol* 269: 1008–1021.
- Schoch RR. 2006. Skull ontogeny: Developmental patterns of fish conserved across major tetrapod clades. *Evol Dev* 8:524–536.
- Sheil CA. 2003. Osteology and skeletal development of *Apalone spinifer* (Reptilia: Testudines: Trionychidae). *J Morphol* 256: 42–78.
- Sheil CA. 2005. Skeletal development of *Macrochelys temminckii* (Reptilia: Testudinea: Chelydridae). *J Morphol* 263: 71–106.
- Sheil CA, Greenbaum E. 2005. Reconsideration of skeletal development of *Chelydra serpentina* (Reptilia: Testudinata: Chelydridae): Evidence for intraspecific variation. *J Zool* 265: 235–267.
- Sheil CA, Portik D. 2008. Formation and ossification of limb elements in *Trachemys scripta* and a discussion of autopodial elements in turtles. *Zool Sci* 25:622–641.
- Shubin NH, Alberch P. 1986. A morphogenetic approach to the origin and basic organization of the tetrapod limb. *Evol Biol* 5:319–381.
- Taylor WR, Van Dyke GC. 1985. Revised procedures for staining and clearing small fishes and other vertebrates for bone and cartilage study. *Cybiurn* 9:107–119.

- Tokita M, Kuratani S. 2001. Normal embryonic stages of the Chinese softshelled turtle *Pelodiscus sinensis* (Trionychidae). *Zool Sci* 18:705–715.
- Tulenko FJ, Sheil CA. 2006. Formation of the chondrocranium of *Trachemys scripta* (Reptilia: Testudines: Emydidae) and a comparison with other described turtle taxa. *J Morphol* 268:127–151.
- Velhagen WA. 1997. Analyzing developmental sequences using sequence units. *Syst Biol* 46:204–210.
- Vogel P. 1972. Vergleichende Untersuchung zum Ontogenesemodus einheimischer Soriciden (*Crocidura russula*, *Sorex araneus* und *Neomys fodiens*). *Revue Suisse de Zoologie* 79:1201–1332.
- Weisbecker V, Goswami A, Wroe S, Sánchez-Villagra MR. 2008. Ossification heterochrony in the mammalian postcranial skeleton and the marsupial-placental dichotomy. *Evolution* 62:2027–2041.
- Werneburg I, Sánchez-Villagra MR. 2009. Time of organogenesis support basal position of turtles in the amniote tree of life. *BMC Evol Biol* 9:82
- Zangerl R. 1969. The turtle shell. In: Gans C, Bellairs Ad'A, Parsons TS, editors. *Biology of the Reptilia*. Vol. 2 Morphology A. London: Academic Press. pp 311–339.
- Zardoya R, Meyer A. 2001. The evolutionary position of turtles revised. *Naturwissenschaften* 88:193–200.
- Ziermann J. 2008. Evolutionäre Entwicklung larvaler Cranialmuskulatur der Anura und der Einfluss von Sequenzheterochronien. Dissertation, Biologisch-Pharmazeutische Fakultät der Friedrich-Schiller-Universität Jena. 332 pp.
- Zusi RL. 1993. Patterns of diversity in the avian skull. In: Hanken J, Hall BK, editors. *The Skull*, Vol. 2. Chicago: Chicago University Press. pp 391–437.